IEEE Access
Multidisciplinary | Rapid Review | Open Access Journal

Received December 18, 2020, accepted January 11, 2021, date of publication January 21, 2021, date of current version January 29, 2021.

Digital Object Identifier 10.1109/ACCESS.2021.3053490

Robotic Tree-Fruit Harvesting With Telescoping Arms: A Study of Linear Fruit Reachability Under Geometric Constraints

RAJKISHAN ARIKAPUDI, (Member, IEEE), AND STAVROS G. VOUGIOUKAS, (Senior Member, IEEE)
Department of Agricultural and Biological Engineering, University of California at Davis, Davis, CA 95616, USA
Corresponding author: Rajkishan Arikapudi (rarikapudi@ucdavis.edu)

This work was supported by USDA-NIFA under Grant 2016-67021-24532.

ABSTRACT Modern commercial orchards are increasingly adopting trees of SNAP architectures (Simple, Narrow, Accessible, and Productive) as the fruits on such trees are, in general, more easily reachable by human or robotic harvesters. This article presents a methodology that utilizes three dimensional (3D) digitized computer models of high-density pear and cling-peach trees, and fruit positions to quantify the linear fruit reachability (LFR) of such trees, i.e., their reachability by telescoping robot arms. Robot-canopy non-interference geometric constraints were introduced in the simulator, to determine the closest position of the arms' base frames with respect to the trees, inside an orchard row. Also, design constraints for such arms, such as maximum reach, size and type of the gripper, and range of approach directions, were introduced to estimate the effect of each of these constraints on the LFR. Simulations results showed that 85.5% of pears were reachable after harvesting consecutively, at three different approach angles ('passes') with a gripper of size 11 cm and an arm extension of 150 cm. For peaches, after three passes, 83.5% were reachable with a gripper size of 11 cm and an arm extension of 200 cm. LFR increased as the gripper's size approached the maximum fruit size and decreased thereafter. Also, retractive grippers on linear arms yielded more fruit compared to vacuum-tube type grippers. Overall, the results suggested that telescoping arms can be used to harvest certain types of SNAP-style trees. Also, this methodology can be used to guide the design of robotic harvesters, as well as the canopy management practices of fruit trees.

INDEX TERMS Computer simulation, harvest efficiency, linear fruit reachability, mechanization, robotic harvesting, telescopic arms.

I. INTRODUCTION

Manual harvesting is one of the most labor-intensive and costly operations in fresh-market fruit production [1]–[3]. Additionally, growers have to depend on a large seasonal semi-skilled immigrant workforce, which is becoming less available [4], [5]. The gradual reduction of farm labor and an increase in tree fruit acreage to meet demand has been reported to result in incomplete fruit harvest and is expected to worsen in the future [6]. Therefore, mechanization is the way to increase worker's productivity [7]. Mechanical harvesting for fresh-market fruits at commercial scale has remained an elusive target. Mass harvesting approaches that include trunk shaking, limb shaking, and canopy contact systems result in unacceptable quantities of damaged fruits, and, in some cases, may cause tree damage as well [8]–[10]. Research done using shake-catch harvesters demonstrated the feasibility of harvesting peach trees trained to either open center or ''Y'' architectures, with damage levels comparable to hand-harvest when the peaches were very firm (not fully mature) [11], [12]. However, the necessity of multiple pickings and the mass removal process which leaves either too many overripe or under-ripe fruit, or both, prevented the commercial adoption of such systems for fresh market harvest. Next, orchard platforms/ harvest aids were developed by researchers [13], [14] and commercial companies [15]–[17] that reduce worker movement between ladders and bins by positioning the worker and bin on a raised platform. Research done on worker productivity using platforms in narrow-inclined trellises showed a 44% increase

The associate editor coordinating the review of this manuscript and approving it for publication was Hiram Ponce.

over conventional hand harvesting [18], whereas research done in open vase training systems resulted in no improvement [19]. However, these machines are not widely adopted in commercial orchards since their productivity is limited due to 1) non uniform fruiting in the canopy which can cause pickers to be idle; 2) unproductive time for picker positioning; 3) variability in worker speeds and 4) inefficiencies due to sub-optimal tree training systems (e.g., wide canopies, hard to reach fruits).

The only remaining option, selective robotic harvesting, is still at a pre-commercial stage, despite active research for at least 30 years [20]–[22]. To a large extent, this lack of progress can be attributed to robots' low cost-effectiveness (high harvest cost) and the inability to harvest a wide range of tree architectures [22]. The three parameters that most heavily influence harvest cost per robot arm are [23]: fruit picking efficiency (FPE), i.e., the ratio of fruits successfully picked over the total number of harvestable fruits; harvester purchase price (HPP); and fruit pick cycle time (PCT), i.e., the average number of seconds between successive fruit picks. Spherical and cylindrical-type robots with extending arms have been developed and tested by researchers in the past [24], [25]. Their use in orchard trees of traditional canopy architectures with large, open-vase, or elliptical-shaped canopies could not achieve FPEs and PCTs that justified commercialization; many fruits in such trees are simply not visible or difficult to reach. Robotic harvesters with multi-degree of freedom revolute-joint arms have also been built [21]. The hypothesis was that, as branches constrain fruit reachability, high kinematic dexterity is necessary for robot arms to navigate through branches and reach fruits inside the canopy [26]. Overall, reported FPEs in literature for single-arm robots harvesting apple or citrus trees range anywhere from 50% to 84%, and PCTs (per fruit, not averaged) range from 3 to 14.3s [21]. The values of these parameters are based on very limited (often unreported) numbers of experiments and picked fruits, using conventional trees, i.e., non-trellised trees with large canopies.

In general, the performance of robotic harvesters depends on the interrelationships among orchard layouts, tree canopy structures, and spatial fruit distributions with harvester mechanics [22]. In an effort to simplify the harvesting task, and increase fruit visibility and reachability, growers have been increasingly adopting high-density SNAP (Simple, Narrow, Accessible, and Productive) tree architectures [27]. Such orchards feature narrow, almost two-dimensional canopies (e.g., tall and super spindle apple orchards) that create ''fruiting walls,'' which are easier to harvest manually, either with ladders, orchard platforms [28] or robots.

An interesting observation is that when multiple perspective views of the canopy are available, a large percentage of fruits may be visible from outside the canopy (up to 91%, compared with 40-70% for single view, for citrus trees [29]). However, being visible also means that fruits are reachable by moving on a straight line. Based on this realization, and on the fact that linear, telescoping arms are less complicated, cheaper, and easier to deploy in large numbers - due to their simple workspace - than multi-degrees of freedom (DOF) revolute joint arms, an approach that is regaining popularity – in modern SNAP-style tree orchards - is to build robotic harvesters that comprise of many 3-DOF telescoping arms [30]. However, we currently lack the tools to evaluate the performance – and thus guide the design - of linear multi-arm robot harvester designs in given types of orchards.

The goal of this work is to develop a methodology that estimates reachability metrics of harvesters using linear arms for fruit trees grown under different training systems. To do this, physics engines that could simulate certain physical systems such as rigid bodies, soft bodies and fluids or combinations of these systems to produce physically plausible scenes are needed. Bullet Physics Library, PhysX, Open Dynamics Engine (ODE) and Havok are amongst the physics engines that are widely available [31]. The Bullet physics library is free, open source and cross-platform software, making it very simple to work with any platform. Therefore, in this study the ray tracing algorithm in Bullet physics was used (with rays originating from sample points on fruit surfaces) to test for linear reachability, and geometric object modelling from the Bullet package was used to model fruits and branches, and check for fruit-to-branch interference (by checking ray-object intersections). So, the goal is to estimate the maximum number of fruits that a linear arm harvester can reach, and not to predict the number of fruits harvested in a real harvesting operation, or how fast the pick cycle would be, metrics that would require dynamic simulation, provided by packages such as V-REP [32], or Gazebo [33], etc. In addition, if simple linear arms could reach majority of the fruit,the need of a complex robotic arm to harvest fruit trees where obstacle detection and avoidance algorithms are needed in fruit harvesting can be avoided.

In this article, 3D digitized computer models of high-density pear and cling peach trees and fruit positions were used to quantify the reachability of fruits in SNAP-type trees, when linear arms are used for harvesting using simple raytracing algorithm from the bullet physics engine. The physics engine is the simplest way to determine fruit reachability as there is no need to model the robotic arms and write control algorithm as in case of a dynamic harvesting simulation. The geometry related to the tree canopy and fruits can be introduced using objects to the world like spheres, boxes, cylinders, capsules, cones, and polyhedrons. To determine machine interface, planes can be added to design constraints for the robotic arms such as maximum reach and to define the closest position of the harvesting machine with respect to the harvested tree. Also, size and type of the gripper, and range of approach directions, and their effects on fruit reachability can be studied using simple ray-tracing algorithms. This methodology can be used to guide the design of robotic harvesters, as well as the canopy management practices of fruit trees.

II. BACKGROUND

The concept of Linear Fruit Reachability (LFR) was formally introduced in [34] and is summarized next. Individual linear fruit reachability was defined as a Boolean variable that is zero if the projection of any point on the fruit's surface along an approach direction vector **d**results in a collision with a branch or the ground before reaching a plane that is vertical to **d**, at a distance farther than the longest branch; otherwise, it is one. This definition corresponds to reachability with an extension motion when a telescoping robot arm reaches out to fruit to pick it; hence, it was referred to as ''linear reachability.'' Fruit-to-fruit collisions were not included in this definition of reachability, because in a real harvesting scenario a fruit occluding other fruits along direction **d** would be picked first since it would be closer to the 'harvesting' side; therefore, it would not present as an obstacle. Also, in this research, our approach calculates the maximum number of fruits that a linear arm could reach which is used as a performance metric for design and not to predict the harvester efficiency. However, in a real case harvesting scenario when ripe fruits are occluded by green fruits, the robot would pick fewer fruits than the maximum number allowed by its design.

Linear fruit reachability LFR(**d**) was defined as the total number of linearly reachable fruits on a number of trees in a particular approach direction **d**, divided by the total number of fruits. The linear fruit reachability LFR($\mathbf{d}_1$; $\mathbf{d}_2$; …; $\mathbf{d}_{i-1}$; $\mathbf{d}_i$) for the *i*th ''harvesting pass'' along a direction $\mathbf{d}_i$ was also defined as the linear fruit reachability of the fruits remaining on the tree, after fruits that were reachable along vectors $\mathbf{d}_1$, $\mathbf{d}_2$, …, $\mathbf{d}_{i-1}$ were removed. Finally, the cumulative linear fruit reachability CLFR($\mathbf{d}_1$, $\mathbf{d}_2$, …, $\mathbf{d}_K$) was defined as the total number of fruits that were linearly reachable after K consecutive ''harvesting passes.'' By definition:

$$CLFR(\mathbf{d}_1,\mathbf{d}_2,\ldots,\mathbf{d}_K) = LFR(\mathbf{d}_1) + LFR(\mathbf{d}_1;\mathbf{d}_2) + \ldots + LFR(\mathbf{d}_1;\mathbf{d}_2;\ldots.\mathbf{d}_K) \quad (1)$$

The above definitions and the analysis performed in [29] did not take into account robot or tree-specific geometric or kinematic constraints. In reality, a fruit that is linearly reachable because all the points on its surface lie on the line-of-sight of the robot gripper, at a given approach angle, may not be reachable because of physical constraints.

This article extends the concept of linear reachability by introducing geometric constraints related to the canopy and machine interference, and design constraints for the robotic arms, such as maximum reach, size and type of the gripper, and range of approach directions. Telescoping-type arms are assumed, and digitized models of high-density pear trees, and V-trellised cling peach trees with fruits are used to estimate 1) the constrained linear reachability of fruits (LFR) 2) the effects of the gripper size, arm extension, and direction of approach parameters of the robotic arm on LFR.

FIGURE 1. Vacuum-tube type gripper that transports the harvested fruit to a bin via the vacuum tube (abundant robotics harvester; photo courtesy of TJ mullinax/good fruit grower).

III. INTRODUCTION OF LINEAR REACHABILITY CONSTRAINTS

First, the effect of the gripper type and size on the fruit linear reachability is studied. The gripper size has a significant impact on the LFR, as the rigid branches act as obstacles that prevent the gripper and arm from reaching to and retracting from the fruit in the canopy. Two established gripper design – and harvesting - approaches are considered. In the first approach, the gripper's cross-section is smaller than or equal to the smaller dimension of any fruit on the tree, and the plucked fruit is brought to the entry point of a conveyance system by retracting the arm - and gripper - back to a position where the fruit can be released. Such grippers include vacuum grippers with a small cross-section and vacuum strong enough that can hold the biggest fruit [35], and grippers with fingers, which enter the canopy with fingers closed, and open them up - to approximately the size of the fruit - to enclose and detach the fruit [36]. As mentioned above, harvesting with such grippers must include a retracting motion, which slows down picking. However, their smaller size reduces canopy-robot interference, thus, potentially increasing the number of reachable fruits. We refer to such grippers as ''retracting-grippers.'' In the second approach, the gripper is a vacuum tube with a cross-section larger than the expected largest dimension of all fruits (FIGURE 1). We refer to such grippers as ''vacuum-tube'' grippers. Harvesting with vacuum-tube grippers does not require a retracting motion, as the fruit is conveyed to the bin via the vacuum tube, so picking is faster; however, the larger size of the gripper may increase branch-robot interference and reduce the number of fruits that can be reached.

The sequence of steps to harvest the fruit for each of the gripper types is presented below (Fig. 2).

Next, the effect of arm extension length on the fruit linear reachability must be studied. The arm extension has a significant impact on the LFR, as the fruit reaching ability of a given arm depends on the distance of fruits in the canopy from the orchard row, and the extension limits of the arm; longer arms are needed to reach fruits closer to the center of the canopy. However, as the orchard row has limited width, longer arms may not fit within the orchard row. Also, longer arms are heavier and slower and are expected to have a negative effect

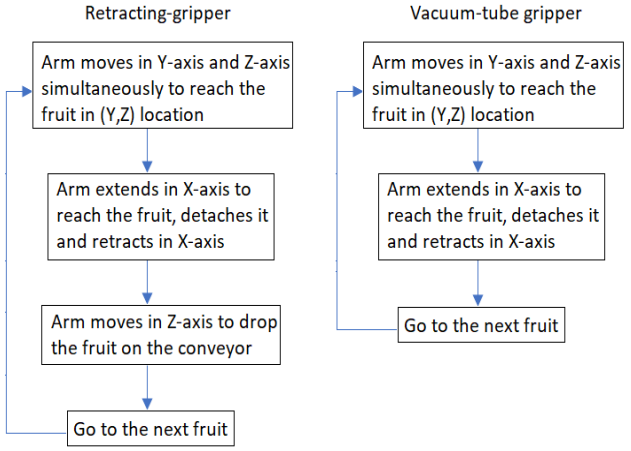

FIGURE 2. Harvest sequence for retracting-gripper and vacuum-tube gripper.

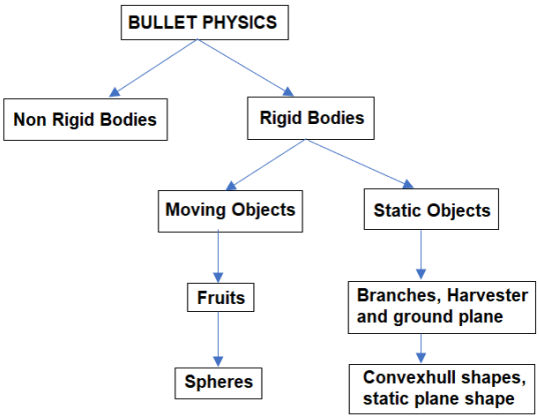

FIGURE 3. Block diagram feauturing the components of bullet physics engine.

on the pick cycle time of the harvester. Therefore, LFR's for arms with different lengths that fit in the orchard row need to be evaluated.

Finally, the effect of the direction of approach of the robotic arm on the fruit linear reachability needs to be studied. Prior research indicated [34] that the majority of the fruits were visible from outside the canopy, which means that these fruits can be reachable from outside the tree canopy using linear motion. However, to reach all the fruits in the canopies, multiple approach angles were needed. Also, the number of fruits reachable varied significantly between approach angles. Therefore, a range of approach angles must be evaluated – in the presence of constraints - to analyze the effect of the approach angle on LFR.

IV. MATERIALS AND METHODS

This section presents the methodology developed to estimate the LFR under constraints using the digitized fruit locations and tree geometries of 20 high-density trellised pear and 20 V-shaped peach fruit trees data set [37], [38]. This data contains branch data and fruit data for 20 pear and 20 peach trees in excel files. Each tree constitutes of several branches split into segments and each segment is represented using conical frustums and each fruit is represented as a sphere. Each row in the excel contains the information of a segment where the first three columns are the center point of the one end of the segment, the fourth column is the radius, the data in columns five to seven are the center point of the other end of the segment and eight column is the radius of the corresponding frustum disc. The ninth column is the branch id to which the segment belongs. In a similar way, the excel files for fruit data has information about the fruit in each row, where the first three columns are the center point of the fruit, the fourth point is the radius of the fruit and fifth point is the branch id to which the fruit belongs.

A. HARVESTING SIMULATOR

1) BULLET PHYSICS

The *Bullet Physics Library* was used to model the harvesting scenario and implement the fruit reachability calculations. The library enables users to create an environment by adding objects to the world like planes, spheres, boxes, cylinders, capsules, cones, and polyhedrons with an arbitrary number of vertices. The objects added to the world can be either fixed or non-fixed. For this research, the tree branches were modeled using polyhedra with N vertices as fixed objects, and the fruits were modeled using spheres as non-fixed objects. The linear fruit reachability was calculated using a ray-tracing algorithm, as explained in the next section. A block diagram is given in Fig. 3 detailing the components and their features.

2) GEOMETRIC REPRESENTATION OF HARVEST ENVIRONMENT

The world frame was defined such that the length of each pear tree was along the Y-axis (row axis), the depth of the tree was along the X-axis, and the height of the tree was on the Z-axis. A picture of the tree is shown in Fig. 4. The current simulation's world includes four types of objects. The first type of object is the ground, which is modeled by a fixed plane that spans the XY-axis. The second type of object is a branch, which is modeled as a fixed polyhedron with N vertices, meant to approximate digitized conical frustums. The third type of object is a fixed plane that spans the YZ-axis, meant to define the closest position of the harvester. The fourth type of object is a fruit, which is modeled by a sphere with radius R_{fruit}. The fruits were approximated as spheres to speed up computations. The largest cross section of each fruit was used to approximate it as a sphere, hence this approach resulted in conservative (lower) estimates for reachability. Ellipses could also be used for more accurate estimates of fruit reachability, at the cost of increased computation. A modeled fruit-tree in the simulator is shown in Fig. 4.

3) FRUIT-BRANCH INTERSECTION CHECKING

The fundamental operation of the LFR estimation algorithm was to calculate whether a gripper (and arm) of a specific circular cross-section could reach a fruit by moving along the direction defined by an approach angle **d.** To do so, ray tracing was used to calculate whether the projection of the

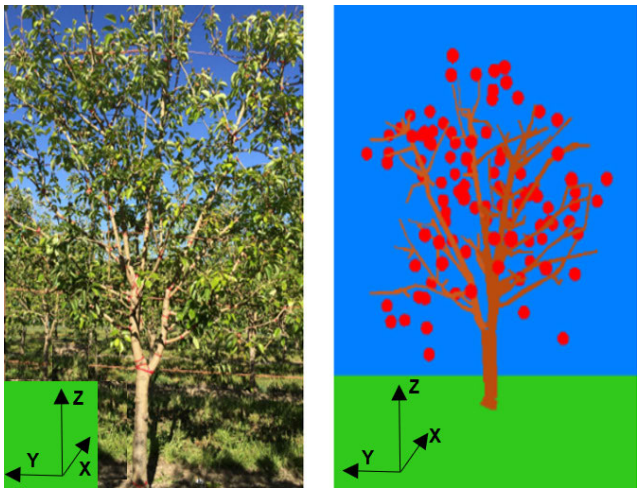

FIGURE 4. Example of the actual and the corresponding digitized/simulated high-density trellised pear tree.

surface of the fruit in the direction of **d**, intersected with any branch. The spherical surface representing the fruit was uniformly sampled, and a ray was shot from each sampled point in the direction of **d**, for a given distance (that is the distance between the center of the tree line to the center of orchard row) If the ray intersected a branch, the fruit was considered as non-reachable through linear motion. Otherwise, the process was repeated for the next sample point, until all points were projected. If no ray hit any branch, then the fruit was said to be reachable.

B. INCORPORATION OF CONSTRAINTS

1) LFR WITH INITIAL GRIPPER POSITION CONSTRAINTS

When considering a harvesting machine in front of a tree inside an orchard row, the initial position of the gripper on a telescoping robotic arm should be farther away than the rigid branch, to avoid branch-robot interference and possible damage (Fig. 5). This distance depends on tree structure and size, and the design of the harvester. The farthest rigid branch located on the tree in the direction perpendicular to the orchard row along the X-axis was defined as the 'initial' position at which the robot arm gripper could be placed in the given orchard row. The farthest rigid branch coordinates on the +X-axis and –X-axis were extracted from the data set. The +X-axis was facing towards the current orchard row, and the -X-axis was facing towards the next orchard row (Fig. 6).

2) LFR WITH ARM EXTENSION CONSTRAINTS

To harvest a tree using a robotic arm, the tree is divided into two halves by the tree line center, assuming that the fruits present on the right side of the tree line center are harvested by the arm when the harvesting machine is in the current orchard row. The fruits on the left side are harvested when the harvesting machine is in the next orchard row (Fig. 7). However, to reach all the fruit, the arm should extend to the tree center line from its initial position in the orchard row. Therefore, the selection of arm extension depends on the

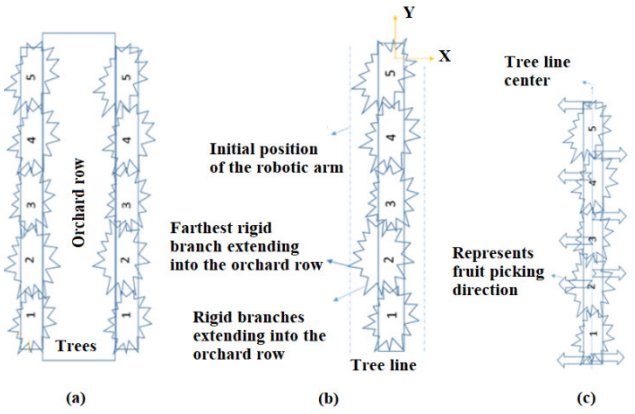

FIGURE 5. Top view of the orchard row showing (a) trees on both sides of the orchard row. (b) harvester positioning and canopy span in the orchard row. (c) fruit picking direction.

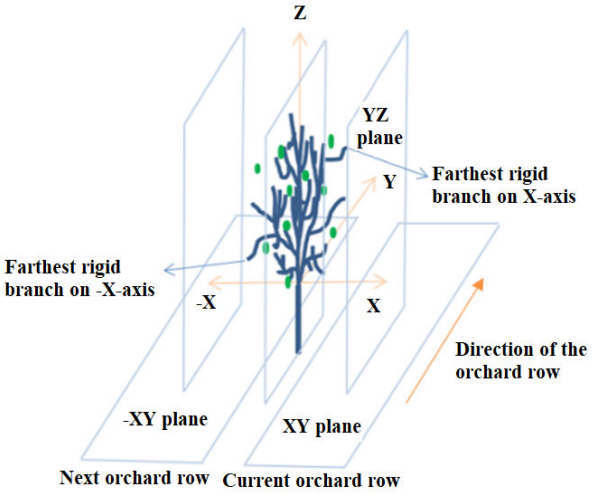

FIGURE 6. Side view of one tree in an orchard row and its orientation in the 3d space.

distance that the arm needs to travel to reach the tree center line from its initial position in the orchard row.

Using the data set for both pear and peach trees, the distance for pears was 100 cm, and peaches were 200 cm. The inter-row distance in pears and peaches was 304.8 cm and 548.6 cm, respectively. Therefore, the space left to position the harvester in the orchard row is 100 cm in pears, and 148.6 cm in peaches. Assuming 100% extension for the arm, the arm could reach the tree center line in pears and peaches. The inter-row spacing of the orchard row, tree line center, along with the distance to the initial position of the arm for pears and peaches, is given in Fig. 8.

To estimate the effect of arm extensions, extensions of 80 cm to 200 cm were used for pears, and 125 cm to 300 cm were used for peaches. To implement maximum arm extension design constraint, a plane in YZ axis was added on both the sides, i.e., in the +ve and -ve X-axis of the tree row, and it defined the position of the harvester. The extension of the arm to reach the fruit in the canopy from the position of the harvester was the same as the distance (D) the fruit

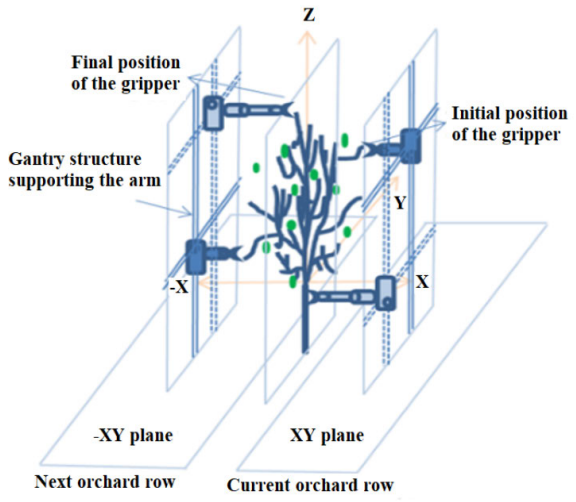

FIGURE 7. Different poses of a robotic arm gripper harvesting a tree in an orchard row.

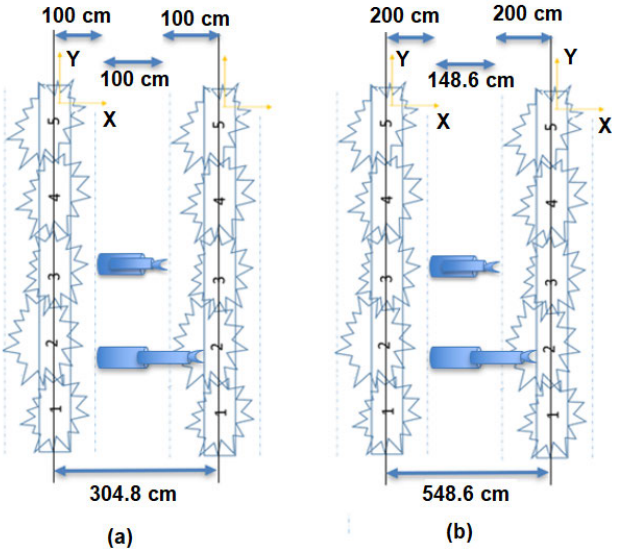

FIGURE 8. Minimum and Maximum retraction length of a Linear arm harvester model in the orchard row (a) Pears; (b) Peaches.

had to travel to reach the YZ plane (Fig. 9). Therefore, each fruit on the tree was projected in the direction of the angle of approach away from the tree on to the YZ image plane. Each time the fruit hit the plane placed in the orchard row, the distance from the fruit to the plane in the direction of the approach was calculated. This gave the distance of the fruit from the harvester, which represented the maximum reach of the arm at that angle of approach from the harvester. Since the robotic arm could not access the fruit from an initial position, which was below the ground based on the given approach angle, a ground plane was added. The fruit was said to be reachable if all the points on the surface of the fruit when projected to an image plane away from the tree didn't hit any tree branch or the ground plane before hitting the planes placed in the tree row. This simulation assumed that all the

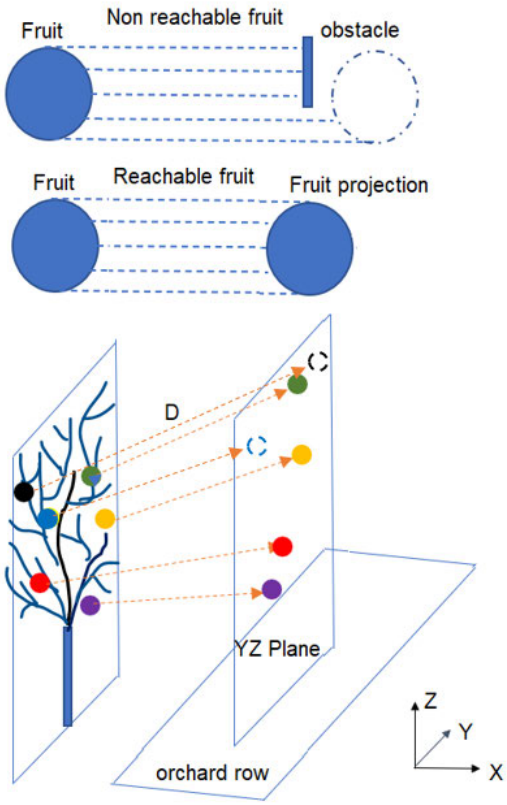

FIGURE 9. Reachable and non-reachble fruit.

fruits that were reachable from above the canopy at a given approach angle could be harvested and did not impose any design constraints on the top plane. The same concept was used to estimate reachabilities for an arm with extensions of 80 cm to 200 cm for pears and 125 cm to 300 cm for peaches.

3) LFR WITH GRIPPER CONSTRAINTS

The selection of gripper depends on the size of the fruit that the gripper needs to grasp. Therefore, the maximum and average size of the pear and peach fruits were extracted from the data set. For pears, the maximum and average fruit length was 11.1 cm and 8.4 cm, respectively, whereas the maximum and average width was 9.5 cm and 7.2 cm, respectively. Therefore, to grasp the largest pear fruit along the length, the gripper needed to be 12 cm in size and to grasp the average fruit, the gripper needed to be 9 cm. For peaches, the maximum size of the fruit was 10.4 cm, and the average size was 6.9 cm. Therefore, to grasp the largest peach fruit, the gripper needed to be 11 cm in size, and to grasp the average fruit, the gripper needed to be 7 cm. The gripper size constraint was implemented in the simulator by changing the size of the fruit while projecting in an image plane to check for collision, as the collision of the fruit with a tree branch in the angle of approach would be the same as the collision of the gripper with a tree branch in the course of reaching a fruit during harvesting.

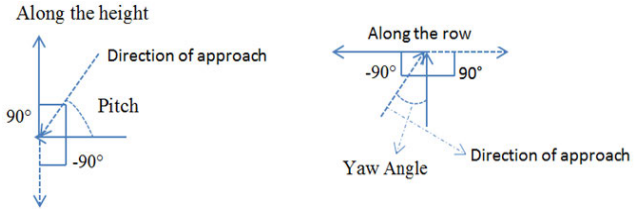

FIGURE 10. The direction of approach of the robotic arm.

To estimate the LFR in the first case, i.e., with a retracting-gripper, the fruits in the data set were projected to the orchard row retaining their sizes, and the reachabilities were estimated. To estimate the LFR in the second case, i.e., with a specific size for the vacuum-tube gripper, all the fruits that were bigger than the size of the vacuum-tube gripper were removed from the data set. Next, the remaining fruits were modeled with their location and the size of the vacuum tube, and the fruits were projected towards the orchard row. The fruits that did not hit the rigid branches were estimated to determine the number of reachable fruits. The same concept was used to estimate reachabilities for an arm with gripper sizes ranging from 7 cm to 15 cm.

4) EFFECT OF APPROACH ANGLE ON LFR

In this analysis, LFR was estimated as a function of the direction of approach. A range of approach angles was derived for the unit vector **d** defined by two angles: an azimuth/Yaw angle, α, about the Z-axis, and an elevation/zenith angle, θ, around the Y-axis. Yaw was -90° along the –Z-axis and 90° along the Z-axis. Elevations ranged from -90° to 90°, and were defined as 0° along the X-axis, and increased clockwise.

To estimate the reachability analysis using the direction of approach, the fruits in the tree canopy were projected towards an imaginary plane along the direction of approach. The imaginary planes that were used to estimate the effect of arm extension were tilted in the direction of approach to determine the effect on fruit reachability. The above process was repeated for different combinations of elevation and azimuth angles to find the best angle(s). The same process was repeated for different design constraints, i.e., max reach and the gripper size of the robotic arm. The LFR was defined as the number of fruits that did not collide with a branch or the ground before colliding with a plane in all K trees divided by the sum of fruits in all K trees. Twenty pear and peach trees were used to estimate the reachability metrics. A set of flowcharts illustrating the fruit reachability procedure are presented next.

Tree structure modeling: The first step is to model the tree with all the digitized branch information. A flowchart illustrating the modeling of the tree structure is presented in Fig. 11.

Fruit modeling: The fruits are modeled based on the gripper type selection as illustrated in section IV.B.3. A flowchart illustrating the modeling of the fruits is presented in Fig. 12.

Fruit reachability: The reachability estimation is done in 2 steps. In the first step, using the approach angle, the distance traveled by the fruits that did not collide with any tree branches as illustrated in section IV.B.4 is recorded. In the final step, given the arm extension, the fruits that are in the reach of the arm are said to be reachable as illustrated in section IV.B.2. A flowchart illustrating the procedure to estimate the reachability given the modeled tree structure, gripper type, direction of approach and arm extension is given in Fig. 13.

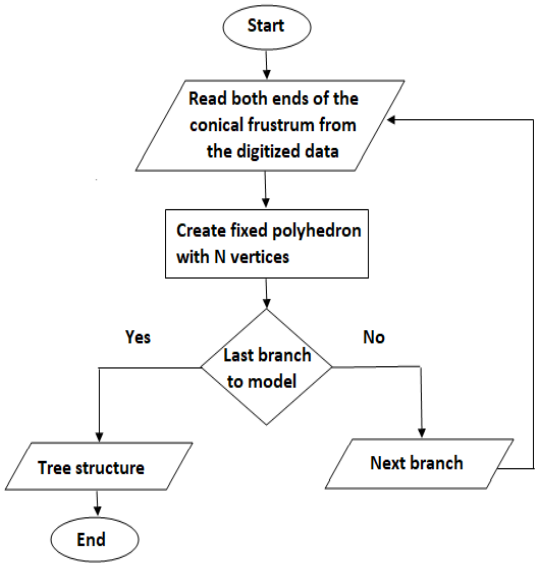

FIGURE 11. Flowchart illustrating procedure to model the tree structure.

5) CUMULATIVE LINEAR FRUIT REACHABILITY (CLFR) AFTER THREE PASSES

In this section, the percentile cumulative linear fruit reachability's (CLFR) for pears and peaches after three passes was estimated using the design constraints of the harvesting actuator, such as maximum reach, gripper cross-section, minimum distance constraint of the machine from the canopy due to branches extending in the row and the direction of approach. During harvest, as the fruits are harvested from the trees, the branches move due to the removal of mass from the tree, which changes the positions of the remaining fruit. However, in this article, the simulation was done under the assumption that the fruit position of unharvested fruit does not change as fruits are being harvested. Later, a side by side evaluation of the LFR obtained for each pass using the harvester models for each training system was presented to determine the feasibility of the harvester model that suits both the tree canopies. To do this, the approach angles that yielded the maximum LFR for each pass and for each variety along with the approach angles that yielded the best LFR for each pass, and both the varieties was obtained.

V. RESULTS

In this section, the effects of gripper size, arm extension, and direction of approach on LFR's are presented for pears

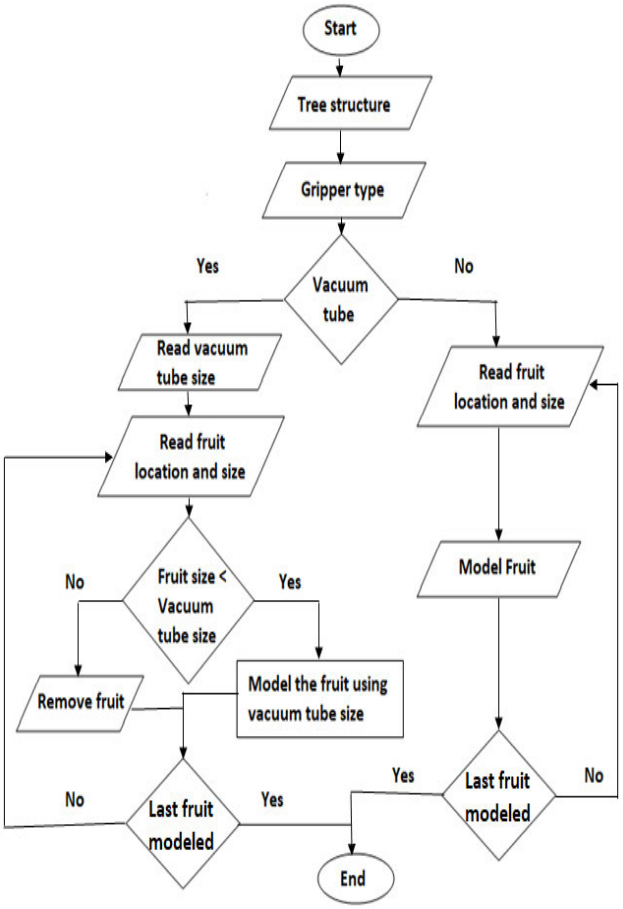

FIGURE 12. Flowchart illustrating the procedure to model fruits.

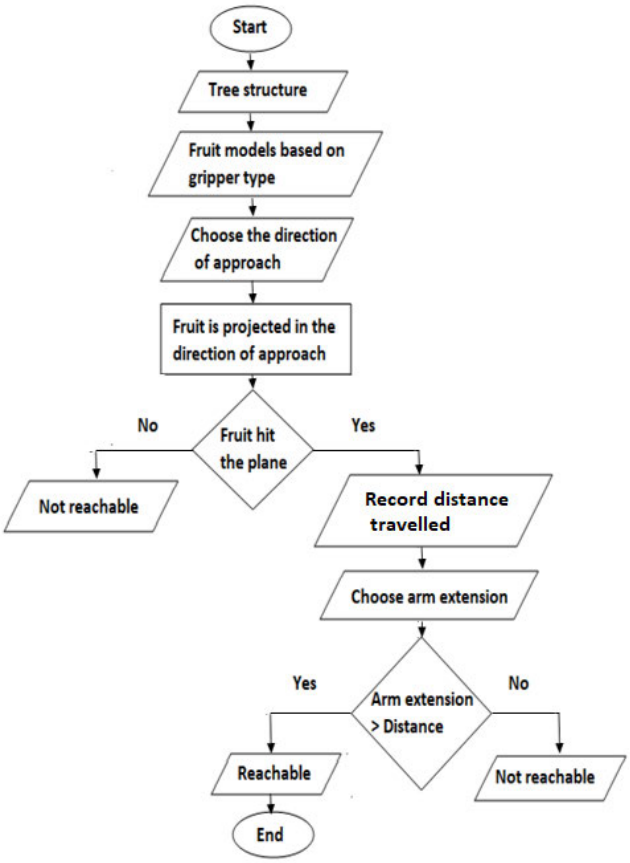

FIGURE 13. Flowchart illustrating the fruit reachability procedure.

and peaches for the first pass. Next, the CLFR for pears and peaches for three passes are presented. Finally, the feasibility of using the same harvester model parameters for both the tree canopies is explored.

A. LFR AS A FUNCTION OF GRIPPER SIZE (CM) IN THE FIRST PASS

In this section, two gripper types are tested. 1) Retracting gripper 2) A vacuum-type tube gripper. For the vacuum-type tube gripper, different sizes of gripper are tested to estimate the effect of gripper size on the LFR. First, the effect on pears is presented, followed by peaches. Later the effect of retracting gripper size on the LFR is presented for pears and peaches.

For a harvester with an arm extension of 150 cm and an approach angle of (0^o, 0^o), the effect of gripper size (7 cm - 15 cm) on the LFR in pears is shown in Fig. 14. The LFR increased as the gripper size increased from 7 cm – 11 cm and dropped when the gripper size increased beyond 12 cm. For a harvester with an arm extension of 200 cm and an approach angle of (0^o, 0^o), the effect of gripper size (7 cm - 15 cm) on the LFR in peaches is shown in Fig. 14. The LFR increased as the gripper size increased from

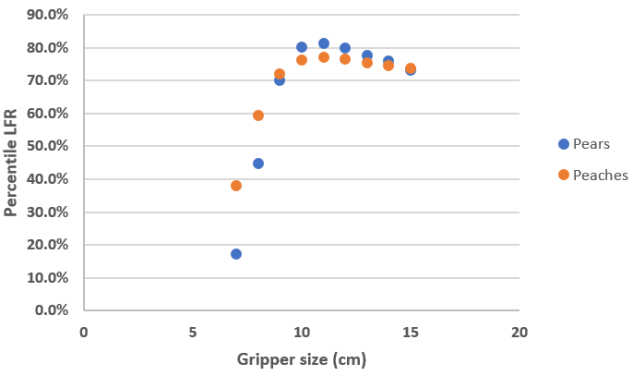

FIGURE 14. Percentile LFR as a function of gripper size of a vacuum-type tube gripper for pears and peaches.

7 cm – 11 cm and dropped when the gripper size increased beyond 12 cm.

The reason is that, as the gripper size became larger, its ability to grasp the bigger fruit increased; however, once the gripper size got bigger than the maximum fruit size on the tree, the gripper collided with more branches while reaching the fruit without any additional gain in fruit grasping. Note that the maximum fruit size from the data collection was 11.1 cm for pears and 10.4 cm for peaches. Therefore, LFR increased as the gripper size increased to fit the maximum

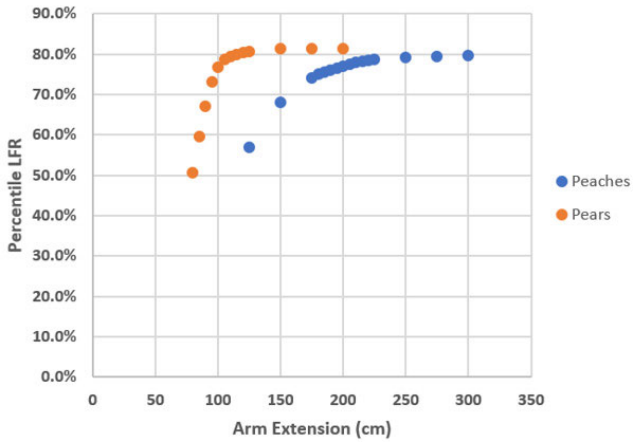

FIGURE 15. Percentile LFR as a function of arm extension for pears and peaches.

fruit size of approximately 11 cm in this research. For vacuum grippers, the percentile LFR's for various gripper sizes are given in Fig. 14 for pears and peaches. The gripper with 11 cm size yielded the highest LFR percentile of 77% for peaches and 81.3% for pears.

For a harvester with an arm extension of 150 cm and approach angle of (0^o, 0^o), the effect of retracting gripper size on the LFR in pears and for a harvester with an arm extension of 200 cm and approach angle of (0^o, 0^o), the effect of retracting gripper size on the LFR in peaches is presented in this section. Simulation analysis showed that 89% of pear fruits and 82.3% of peach fruits were linearly reachable using retracting gripper, which implied that retracting grippers yielded 8% more pears and 5% more peaches when compared to vacuum grippers. The retracting gripper is meant to have the ability to grasp both the small and big fruit and bore its size as the fruit size it grasped. Due to its adaptability in size, while reaching the fruit and retracting, the gripper collided with branches fewer times, which increased its reachability to the majority of the fruits.

B. LFR AS A FUNCTION OF MAXIMUM ARM EXTENSION (CM) IN THE FIRST PASS

In this section, different lengths of maximum arm extension are tested to estimate their effect on the percentile LFR for pears and peaches. The results are presented in Fig. 15. First, the effect of arm extensions (80 cm to 200 cm) on the LFR in pears using a harvester with a retracting gripper size of 11 cm, approach angle of 0^o, 0^o is presented. The LFR decreased as the maximum arm extension decreased because the arm could not reach the fruits that were deep inside the canopy. The LFR for pears dropped dramatically when the arm extension decreased below 100 cm because the distance from the tree centerline to the harvester position was 100 cm, and therefore when the arm extension was below 100 cm, the arm could not reach the fruit present near the center of the canopy. Next, the effect of arm extensions (125 cm to 300 cm) on the LFR in peaches using a harvester with a gripper size of 11 cm, approach angle of 0^o, 0^o is presented. The LFR decreased as the maximum arm extension decreased because the arm could not reach the fruits that were deep inside the canopy. In peaches, the distance from the tree centerline to the harvester position was 200 cm. As the arm extension decreased below 200 cm, the drop in fruit reachability was not as steep when compared to pears because of the V-shaped tree architecture. Also, longer arm extensions were used in peaches compared to pears to reach fruits due to the V-shaped tree architecture.

C. LFR AS A FUNCTION OF APPROACH ANGLE IN THE FIRST PASS

In this section, different angles of approach are tested to estimate the effect of the approach angle on the LFR in the first pass. First, the effect on pears is presented, followed by peaches. For a harvester with retracting gripper size, arm extension of 150 cm, the effect of approach angle (-90^o, 90^o) on the LFR in pears is presented. The LFR percentile was maximum for angle pair (0^o, -10^o) with 81.8%. Also, for this range of angles (-30^o to 30^o) for pitch and yaw, the LFR was not significantly different than the angle pair with the maximum LFR, as shown in FIGURE 16. For a harvester with retracting gripper size, arm extension of 200 cm, the effect of approach angle (-90^o, 90^o)on the LFR in peaches is presented. The percentile LFR was maximum for angle pair (-10^o, 0^o) with 77.7%. Also, for this range of angles (-30^o to 30^o), the LFR was not significantly different than the angle pair with the maximum LFR, as shown in Fig. 16. The LFR decreased outside these boundaries for both pears and peaches.

A means test was conducted for pears, and the p-value was > 0.05 for angle pair ranges (-30^o to 30^o) indicating that there was no significant difference between these angle pair ranges with the maximum LFR and when the boundary for angle pair increased to include -40^o and 40^o, the p-value was < 0.05 indicating that the LFR was significantly different than the angle pair with the maximum LFR for pears as shown in TABLE 1.

A means test was conducted for peaches, and the p-value was > 0.05 for angle pair ranges (-30^o to 30^o) indicating that there was no significant difference between these angle pair ranges with the maximum LFR and when the boundary for angle pair increased to include -40^o and 40^o, the p-value was < 0.05 indicating that the LFR was significantly different than the angle pair with the maximum LFR for peaches as shown in TABLE 2. The reason was that as the pitch angle increased beyond 30^o or decreased beyond -30^o the arm had greater chances interfering with the top or bottom branches and also the increase in angle reduced the horizontal (X-axis) reach of the arm into the canopy which reduced the range of the arm span in Z-axis thereby reaching less number of fruit.

In the first pass, all the fruits in the data set were checked for linear reachability using different angle pairs ranging between (-90^o to 90^o). The angle pair that obtained the

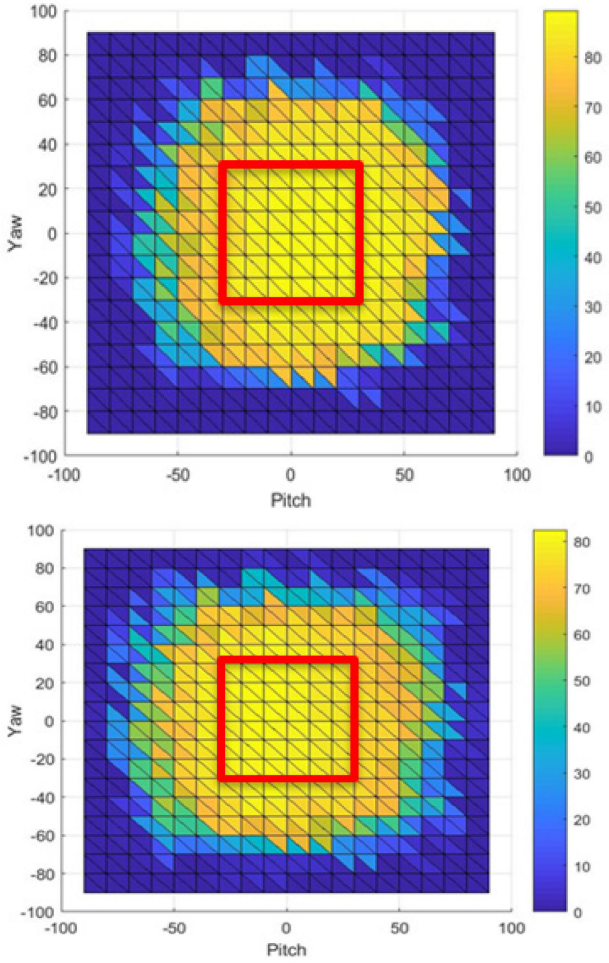

FIGURE 16. LFR as a function of the direction of approach; Pears (top), Peaches (bottom).

TABLE 1. Results of t-Test for Pears for LFR as a Function of the Direction of Approach.

Angle pair -30° ≤ pitch ≤ 30° -30° ≤ yaw ≤ 30° t-Test: One-Sample assuming unequal variances	
	LFR
Mean	78.92
Variance	5.62
Observations	49
Maximum LFR	81.8
Df	3
t Stat	1.88
P(T≤t) one-tail	0.07
t Critical one-tail	2.35
P(T≤t) two-tail	0.16
t Critical two-tail	3.18

Angle pair -40° ≤ pitch ≤ 40° -40° ≤ yaw ≤ 40° t-Test: One-Sample assuming unequal variances	
	LFR
Mean	76.87
Variance	21.24
Observations	81
Maximum LFR	81.8
df	3
t Stat	3.10
P(T≤t) one-tail	0.03
t Critical one-tail	2.35
P(T≤t) two-tail	0.05
t Critical two-tail	3.18

maximum LFR in the first pass was defined as the first approach angles. The fruits that were not reachable in the first pass were checked for reachability using different angle pairs ranging between (-90° to 90°), and the angle pair

TABLE 2. Results of t-Test for peaches for LFR as a function of the direction of approach.

Angle pair -30° ≤ pitch ≤ 30° -30° ≤ yaw ≤ 30° t-Test: One-Sample assuming unequal variances	
	LFR
Mean	73.43
Variance	11.24
Observations	49
Maximum LFR	77.74
Df	4
t Stat	0.80
P(T≤t) one-tail	0.23
t Critical one-tail	2.13
P(T≤t) two-tail	0.47
t Critical two-tail	2.78

Angle pair -40° ≤ pitch ≤ 40° -40° ≤ yaw ≤ 40° t-Test: One-Sample assuming unequal variances	
	LFR
Mean	68.94
Variance	52.51
Observations	81
Maximum LFR	77.74
Df	92
t Stat	-2.94
P(T≤t) one-tail	0.0
t Critical one-tail	1.66
P(T≤t) two-tail	0.0
t Critical two-tail	1.99

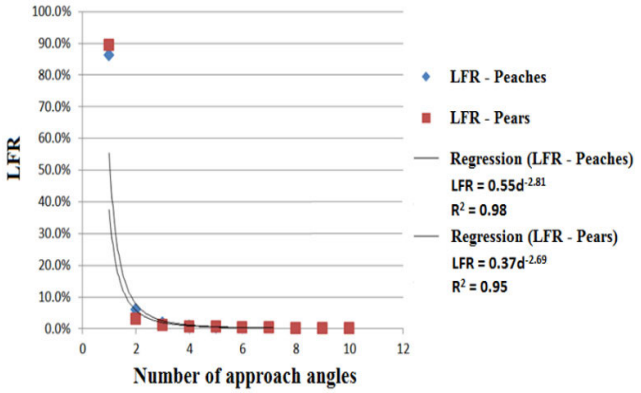

FIGURE 17. Percentile LFR as a function of approach angles for pears and peaches.

that obtained the maximum LFR for the second pass was noted. This was the LFR for the second approach angles. The process was repeated by checking the reachability of the remaining non-reachable fruits from the previous passes using different angle pairs ranging between (-90° to 90°), and the angle pair that obtained the maximum LFR was noted for the next passes as shown in Fig. 17. Also, simulation analyses show that percentile LFR followed a decaying power law as a function of a number of consecutive approach angles.

D. CONSTRAINED CLFR AFTER THREE PASSES

The percentile LFR for three individual passes using the arm with an extension of 150 cm, a gripper size of 11 cm, and the best approach direction for pears are discussed in this section. In the first pass, the maximum percentile LFR was calculated to be 81.8% and was achieved from an elevation angle of 0° and azimuth angle of -10°. It corresponded to 2390 reachable pears out of 2922 in total. The 2390 reachable pears from the first pass were removed from the trees, and reachability was calculated for the remaining 532 fruits. In the second pass, the maximum percentile LFR was calculated to be

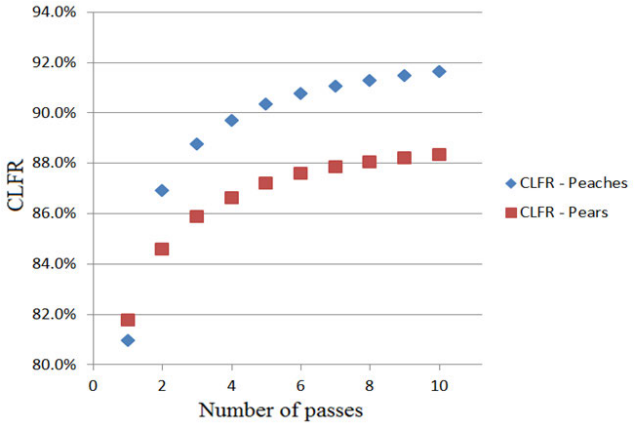

FIGURE 18. CLFR as a function of the number of passes for pears and peaches for a vacuum-type tube gripper of size 11 cm.

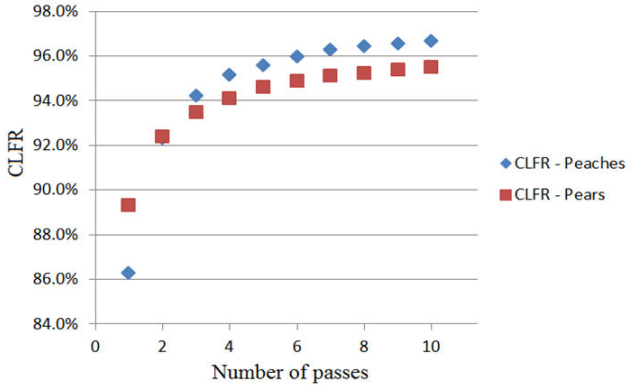

FIGURE 19. CLFR as a function of the number of passes for pears and peaches for the retracting grippe.

2.5% and was achieved from an elevation angle of -20° and azimuth angle of 40°. It corresponded to 72 reachable pears out of 2922 in total. For the third pass, the fruits that were reachable in the first and second passes were removed from the trees, and the reachability was calculated for the remaining 460 fruits. In the third pass, the maximum percentile LFR was calculated to be 1.2% and was achieved from an elevation angle of 10° and azimuth angle of -40°. It corresponded to 35 reachable pears out of 2922 in total. Therefore, the CLFR, after three passes, was 85.5% for pears.

The percentile LFR for three individual passes using the arm with an extension 200 cm, gripper size 11 cm, and the best approach direction for peaches are discussed in this section. In the first pass, the maximum LFR was calculated to be 77.7% and was achieved from an elevation angle equal to −10° and azimuth angle at 0°. It corresponded to 5379 reachable peaches out of 6920. The reachable peaches from the first pass were removed from the trees, and reachability was calculated for the remaining 1540 fruits. In the second pass, the maximum percentile LFR was calculated to be 3.5% and was achieved from an elevation angle of -20° and azimuth angle of 30°. It corresponded to 243 reachable peaches out of 6920 in total. For the third pass, the fruits that were reachable in the first and second passes were removed from the trees, and the reachability was calculated for the remaining 1297 fruits. In the third pass, the maximum percentile LFR was calculated to be 2.3% and was achieved from an elevation angle of 0° and azimuth angle of -40°. It corresponded to 159 reachable peaches out of 6920 in total. Therefore, the CLFR, after three passes, was 83.6% for peaches.

The CLFR percentile of a vacuum-type tube gripper of size 11 cm as a function of the number of passes for peach and pear fruits are discussed in this section. Results indicated that the percentile CLFR after three passes was 85.5% for pears and 83.6% for peaches as shown in Fig. 18. Also, the CLFR percentile of a retracting gripper as a function of the number of passes for peach and pear fruits are discussed in this section. Results indicate that the percentile CLFR after three passes was 93.3% for pears and 88.9% for peaches as shown in Fig. 19. However, no analysis was done on evaluating the price of this harvester; therefore, the financial benefit of doing multiple passes was not addressed. Also, the cost to harvest may vary depending on factors like the design of the harvester, the value of the fruit, etc.

In this section, the feasibility of using the same harvester model parameters that could perform well with both tree canopies is explored. The scenario that yielded the highest LEV (LFR for each variety), LBV (LFR for both varieties), CLEV (CLFR for each variety) and CLBV (CLFR for both varieties) is listed in TABLE 3, along with the optimal scenario for both varieties using an arm with a gripper size of 11 cm and an arm extension of 200 cm.

TABLE 3. LFR of a Robotic Arm With Vacuum-Tube Gripper Size (11 cm) and Arm Extension (200 cm) in Pears and Peaches for Three Passes, and Two Harvesting Scenarios.

		Pears			Peaches		
	Pass	Pitch	Yaw	LFR	Pitch	Yaw	LFR
LEV	1	0°	-10°	81.8%	-10°	0°	77.7%
LBV	1	0°	0°	81.3%	0°	0°	77.0%
LEV	2	10°	50°	2.8%	-20°	30°	3.5%
LBV	2	-20°	40°	2.7%	-20°	40°	3.4%
LEV	3	50°	-40°	1.2%	0°	-40°	2.3%
LBV	3	-10°	-40°	1.2%	-10°	-40°	2.2%
CLEV	1+2 +3			85.8%			83.5%
CLBV	1+2 +3			85.2%			82.7%

LEV = LFR for best direction of approach for each variety, LBV = LFR for best direction of approach for both varieties, CLEV = CLFR for best direction of approach for each variety, CLBV = CLFR for best direction of approach for both varieties

The results indicate that there was a negligible difference between these two cases, which implies that the direction of approach, the arm extension and gripper size could be fixed for each pass, irrespective of whether a pear or peach tree is being harvested. However, the arm extension lengths selected for pears in Fig. 15 would have negative consequences for peach harvesting, because of the location of fruits in the canopy due to the difference in the tree architecture.

VI. SUMMARY & CONCLUSION

This article presented a simulation study on LFR for digitized high-density trellised pear and high-density V-shaped peach trees when the constraints imposed by arm extension length, approach-angle, and gripper type and size are incorporated. Thin, flexible branches were not included in this study, and their effects are not expected to affect LFR significantly.

The average and maximum fruit size from the data collection was 7.2 cm and 11.1 cm for pears and 6.9 cm and 10.4 cm for peaches. Therefore, to grasp the largest pear and peach fruit, the gripper needed to be 11 cm in size, and to grasp the average fruit, the gripper needed to be 7 cm. The simulation results for both the pear and peach trees showed that for a given approach angle and arm length, LFR increased as the vacuum-tube type gripper size increased from 7 cm to 11 cm, and decreased beyond 11 cm, i.e., *LFR increased as the gripper's size approached the maximum fruit size and decreased after it passed the maximum fruit size.* For pears, a high percentage of fruit (85.5%), were reachable using an arm extension of 150 cm and a gripper size of 11 cm. For peaches, 83.5% of fruits were reachable using an arm extension of 200 cm and a gripper size of 11 cm.

Also, the regression analysis showed that the retracting-gripper yielded 93.3% for pears and 88.9% for peaches, and that *retractive grippers on linear arms yielded more fruit compared to vacuum-tube type grippers* (7.8% for pears and 5.4% for cling peaches).

The knowledge about the LFR for individual passes could be used to determine the type of robot structure that could be used to harvest the fruit on these training systems. LFR and CLFR analyses can help in making economic decisions in the harvester design to determine the harvest cost per fruit for individual passes. Overall, the results of this study suggest that for some trees of SNAP-type architectures, high fruit reachability may not require complex and expensive arms with many degrees of freedom; instead, simpler linear arms can be used.

The same approach can be used to test the reachability metrics of telescopic arms for several fruit trees like apples, plums, nectarines, and persimmons etc., under different training systems. As a next step, throughput analysis of the harvester will be estimated using the reachable fruits, in a simulation that incorporates motion dynamics.

ACKNOWLEDGMENT

We would like to thank numerous California growers for letting us gather data during their busy harvesting season.

REFERENCES

[1] Q. Zhang, *Automation in Tree Fruit Production: Principles and Practice*. Wallingford, U.K.: CABI, 2017.

[2] A. Lewis, L. P. Watts, and B. K. Nagpal, "Investment analysis for robotic applications," Soc. Manuf. Eng., Southfield, MI, USA, Tech. Paper NO 380, 1983.

[3] E. J. van Henten, "Greenhouse mechanization: State of the art and future perspective," *Acta Horticulturae*, no. 710, pp. 55–70, Jun. 2006.

[4] J. E. Taylor, D. Charlton, and A. Yúnez-Naude, "The end of farm labor abundance," *Appl. Econ. Perspect. Policy*, vol. 34, no. 4, pp. 587–598, Dec. 2012.

[5] L. Calvin and P. Martin, "The U.S. Produce industry and labor: Facing the future in a global economy," United States Dept. Agricult. (USDA), Economic Research, Economic Res. Service, Washington, DC, USA, Tech. Rep. No. 106., 2010.

[6] G. Warner, "Tighter borders may be keeping out workers," *Good Fruit Growe*, vol. 54, no. 11, pp. 10–11, 2003.

[7] J. S. Holt, "Implications of reduced availability of seasonal agricultural workers on the labor-intensive sector of U.S. Agriculture," Amer. Soc. Agr. Eng., St. Joseph, MI, USA, Tech. Rep. ASAE Paper #991095, 1999.

[8] D. L. Peterson, B. S. Bennedsen, W. C. Anger, and S. D. Wolford, "A systems approach to robotic bulk harvesting of apples," *Trans. ASAE*, vol. 42, no. 4, pp. 871–876, 1999.

[9] A. Torregrosa, E. Ortí, B. Martín, J. Gil, and C. Ortiz, "Mechanical harvesting of oranges and Mandarins in Spain," *Biosyst. Eng.*, vol. 104, no. 1, pp. 18–24, Sep. 2009.

[10] M. E. De Kleine and M. Karkee, "A semi-automated harvesting prototype for shaking fruit tree limbs," *Trans. ASABE*, vol. 58, no. 6, pp. 1461–1470, 2015.

[11] R. G. Diener, R. E. Adams, P. E. Nesselroad, K. C. Elliott, M. Ingle, and S. H. Blizzard, "Mechanical harvesting of tree fruits in West Virginia," Amer. Soc. Agr. Eng., St. Joseph, MI, USA, Tech. Rep. ASAE Paper No. 76-1953, 1976.

[12] D. L. Peterson and G. E. Monroe, "Continuously moving shake-catch harvester for tree crops," *Trans. ASAE* vol. 20, no. 2, pp. 202–205, 1977.

[13] A. G. Berlage, R. D. Langmo, and G. E. Yost, *Limitations of Single- and Multi-Man Platform Harvesting Aids*. Corvallis, OR, USA: Oregon State Univ., 1972.

[14] D. L. Peterson, "Development of a harvest aid for narrow-inclined-trellis tree-fruit canopies," *Appl. Eng. Agricult.* vol. 21, no. 5, pp. 803–806, 2005.

[15] Anonymous, "Apple harvesting: Dutch machines cut down pickers," *Grower*, vol. 14, no. 11, p. 31, 1981.

[16] Z. Zhang, Z. H. Zhang, X. M. Wang, H. Liu, Y. J. Wang, and W. J. Wang, "Models for economic evaluation of multi-purpose apple harvest platform and software development," *Int. J. Agric. Biol. Eng.*, vol. 12, no. 1, pp. 74–83, 2019.

[17] P. Klassen, "Picking platforms," *Fruit Grower*, vol. 107, no. 10, pp. 6–7, 1987.

[18] D. L. Peterson, S. S. Miller, and S. D. Wolford, "Apple harvest aid for inclined trellised canopies," *Trans. ASAE*, vol. 40, no. 3, pp. 529–534, 1997.

[19] R. B. Elkins, J. M. Meyers, and V. Duraj, "Comparison of platform versus ladders for harvest in northern California pear orchard," in *Proc. 11th Int. Pear Symp., ISHS Acta Horticulturae*, Ventura, CA, USA: Patagonia, 2011, pp. 241–249.

[20] Y. Sarig, "Robotics of fruit harvesting: A state-of-the-art review," *J. Agricult. Eng. Res.*, vol. 54, no. 4, pp. 265–280, Apr. 1993.

[21] C. W. Bac, E. J. van Henten, J. Hemming, and Y. Edan, "Harvesting robots for high-value crops: State-of-the-art review and challenges ahead," *J. Field Robot.*, vol. 31, no. 6, pp. 888–911, Nov. 2014.

[22] S. G. Vougioukas, "Agricultural robotics," *Annu. Rev. Control, Robot., Auto. Syst.*, vol. 2, no. 1, pp. 365–392, May 2019, doi: 10.1146/annurev-control-053018-023617.

[23] R. Harrell, "Economic analysis of robotic citrus harvesting in Florida," *Trans. ASAE*, vol. 30, no. 2, pp. 298–304, 1987.

[24] G. d'Esnon, G. Rabatel, R. Pellenc, A. Journeau, and M. J. Aldon, "MAGALI: A self-propelled robot to pick apples," ASAE, St. Joseph, MI, USA, Tech. Paper 87-1037, 1987.

[25] R. C. Harrell, P. D. Adsit, and D. C. Slaughter, "Real-time vision-servoing of a robotic tree fruit harvester," ASAE, St. Joseph, MI, USA, Tech. Paper 85–3550, 1985.

[26] E. J. Van Henten, E. J. Schenk, L. G. van Willigenburg, J. Meuleman, and P. Barreiro, "Collision-free inverse kinematics of the redundant seven-link manipulator used in a cucumber picking robot," *Biosyst. Eng.*, vol. 106, no. 2, pp. 112–124, Jun. 2010.
[27] M. Karkee and Q. Zhang, "Mechanization and automation technologies in specialty crop production," *Resource Mag.*, vol. 19, no. 5, pp. 16–17, 2012.
[28] R. K. Gallardo and M. P. Brady, "Adoption of labor-enhancing technologies by specialty crop producers: The case of the washington apple industry," *Agricult. Finance Rev.*, vol. 75, no. 4, pp. 514–532, Nov. 2015.
[29] D. M. Bulanon, T. F. Burks, and V. Alchanatis, "Fruit visibility analysis for robotic citrus harvesting," *Trans. ASABE*, vol. 52, no. 1, pp. 277–283, 2009.
[30] J. H. Tibbets, "Not too far from the tree," *Mech. Eng.*, vol. 140, no. 2, pp. 28–33, Feb. 2018.
[31] E. Izadi and A. Bezuijen, "Simulating direct shear tests with the bullet physics library: A validation study," *PLoS ONE*, vol. 13, no. 4, Apr. 2018, Art. no. e0195073.
[32] E. Rohmer, S. P. N. Singh, and M. Freese, "V-REP: A versatile and scalable robot simulation framework," in *Proc. IEEE/RSJ Int. Conf. Intell. Robots Syst.*, Nov. 2013, pp. 1321–1326.
[33] N. Koenig and A. Howard, "Design and use paradigms for gazebo, an open-source multi-robot simulator," in *Proc. IEEE/RSJ Int. Conf. Intell. Robots Syst. (IROS)*, Sep. 2004, pp. 2149–2154.
[34] S. G. Vougioukas, R. Arikapudi, and J. Munic, "A study of fruit reachability in orchard trees by linear-only motion," *IFAC-PapersOnLine*, vol. 49, no. 16, pp. 277–280, 2016.
[35] C. Lehnert, A. English, C. McCool, A. W. Tow, and T. Perez, "Autonomous sweet pepper harvesting for protected cropping systems," *IEEE Robot. Autom. Lett.*, vol. 2, no. 2, pp. 872–879, Apr. 2017, doi: 10.1109/LRA.2017.2655622.
[36] Z. De-An, L. Jidong, J. Wei, Z. Ying, and C. Yu, "Design and control of an apple harvesting robot," *Biosyst. Eng.*, vol. 110, no. 2, pp. 112–122, Oct. 2011.
[37] S. Vougioukas and R. Arikapudi, "Digitized pear and peach trees with fruits, v2, UC Davis," *Dataset*, to be published, doi: 10.25338/B8WW41.
[38] R. Arikapudi, S. Vougioukas, and T. Saracoglu, "Orchard tree digitization for structural-geometrical modeling," in *Proc. 10th Eur. Conf. Precis. Agricult. (ECPA)*, 2015, pp. 329–336.

RAJKISHAN ARIKAPUDI (Member, IEEE) was born in Dosapadu, India, in 1989. He received the B.S. degree in electronics and communications engineering from the V. R. Siddhartha Engineering College, Vijayawada, India, in 2010, the M.S. degree in electrical and electronics engineering from California State University, Fresno, CA, USA, in 2012, and the Ph.D. degree in biological and agricultural engineering from the University of California at Davis, Davis, CA, USA, in 2019.

Since 2019, he has been a Postdoctoral Scholar with the Department of Agricultural and Biological Engineering, University of California at Davis. His research interests include automation, robotic harvesting, yield mapping, and fruit trees modeling.

STAVROS G. VOUGIOUKAS (Senior Member, IEEE) received the Diploma degree in electrical engineering from the Aristotle University of Thessaloniki, Thessaloniki, Greece, in 1989, the M.Sc. degree in electrical and computer engineering from SUNY at Buffalo, in 1999, and the Ph.D. degree in robotics and automation from Rensselaer Polytechnic Institute, in 1995. He conducted graduate studies in the USA under a Fulbright grant and several research assistantships.

Until 2011, he was a Faculty with the School of Agriculture, Aristotle University of Thessaloniki. In 2012, he joined the Biological and Agricultural Engineering Department, University of California at Davis. His research interests include navigation for agricultural robots, robot-aided and autonomous harvesting, and mechanization and automation for specialty crops. He has authored or coauthored more than 120 refereed journal and conference articles in the above areas. Since 2015, he has been serving as an Associate Editor for the *Biosystems Engineering* journal.